

# Resonance and composition effects on the Raman scattering from silver-gold alloy clusters

H. Portales<sup>1,a</sup>, L. Saviot<sup>1</sup>, E. Duval<sup>1</sup>, M. Gaudry<sup>2</sup>, E. Cottancin<sup>2</sup>, J. Lermé<sup>2</sup>, M. Pellarin<sup>2</sup>, M. Broyer<sup>2</sup>, B. Prével<sup>3</sup>, and M. Treilleux<sup>3</sup>

<sup>1</sup> Laboratoire de Physicochimie des Matériaux Luminescents, Université Lyon 1 and CNRS, 69622 Villeurbanne Cedex, France

<sup>2</sup> Laboratoire de Spectrométrie Ionique et Moléculaire, Université Lyon 1 and CNRS, 69622 Villeurbanne Cedex, France

<sup>3</sup> Département de Physique des Matériaux, Université Lyon 1 and CNRS, 69622 Villeurbanne Cedex, France

Received 16 November 2000

**Abstract.** Low-frequency Raman scattering experiments have been performed on thin films consisting of pure gold or gold-silver alloy clusters embedded in alumina matrix. It is clearly shown that the quadrupolar vibrational modes are observed by Raman scattering because of the effect of resonance with the excitation of the electronic surface dipolar plasmon. This is due to the strong coupling between the collective electronic dipolar excitation and the quadrupolar vibrational modes. This effect of resonance does not exist with the core electron excitations. The mixing of the conduction electron dipolar excitation (surface plasmon) with the core electrons leads to the quenching of the resonant Raman scattering.

**PACS.** 36.40.Vz Optical properties of clusters – 36.40.Gk Plasma and collective effects in clusters – 78.30.Er Solid metals and alloys – 36.20.Ng Vibrational and rotational structure, infrared and Raman spectra – 73.61.At Metal and metallic alloys

## 1 Introduction

Silver nanocrystals embedded in dielectric films are currently attracting much interest because of the non-linear optical properties, which are related to the strong absorption in the blue spectrum. This absorption stems from the excitation of the surface dipolar plasmon (collective electronic excitation). A consequence of that is a relatively strong Raman scattering by the quadrupolar vibrational modes of the silver clusters [1–4]. For a spherical cluster, from the selection rules, the only modes visible by Raman scattering are the spherical and quadrupolar ones. The reason why the quadrupolar modes are easily observed by Raman scattering, is that these modes are much more coupled than the spherical one to the dipolar plasmon, as it can be shown by theoretical calculations [5]. The Raman scattering by the quadrupolar modes of silver clusters is, then, resonant.

In silver clusters embedded in dielectric matrices the absorption by the dipolar plasmon excitation is exhausted by the conduction electrons and is well separated from the one corresponding to the core electron excitation (interband transitions). Conversely, for gold clusters the plasmon excitation, in the 450 – 650 nm spectral range, overlaps the low-energy wing of the interband transitions [6],

so that there is a mixing of both excitations. It is interesting, in the one hand, to know if the Raman scattering can be resonant with the core electron excitations, and, on the other hand, to determine the effect of the mixing of both excitations on the Raman scattering from gold clusters.

By laser vaporization, it is possible to deposit films with  $\text{Au}_x\text{Ag}_{1-x}$  alloy clusters of different compositions. In the collective excitations, like the dipolar plasmon, all the conduction electrons, from Ag and Au atoms, are involved without distinction. The energy of the dipolar plasmon in the alloy cluster will depend on the composition  $x$  of the  $\text{Au}_x\text{Ag}_{1-x}$  alloy cluster: It will shift to the red when the Au concentration will increase. In consequence, the overlap of the plasmon excitation with the interband transitions will vary with the composition  $x$  of the  $\text{Au}_x\text{Ag}_{1-x}$  clusters. Thus, by the observation of the Raman scattering from alloy clusters, some information about the effect of the mixing of both electronic excitations on the resonant Raman scattering is expected to be gained.

In this paper, Raman scattering experiments from Au and  $\text{Au}_x\text{Ag}_{1-x}$  clusters of different compositions, by excitation at different wavelengths, are reported. It will be shown that there is no resonant Raman scattering with the core electron excitations, and that the mixing of the dipolar plasmon excitation with the interband transitions diminishes the resonant Raman effect.

---

<sup>a</sup> e-mail: portales@pcml.univ-lyon1.fr

**Table 1.** Position of the low-frequency Raman peak, for an excitation at 514.5 nm, compared with the cluster diameter corresponding to the maximum of the size distribution determined by electron microscopy, for the different composite alumina:  $\text{Au}_x\text{Ag}_{1-x}$  films.

$x$	$\omega$ ( $\text{cm}^{-1}$ )	$D_{max}$ (nm)
1	6.6	2
0.75	9.2	2.1
0.5	11.1	2.3
0.25	10.2	2.3

## 2 Experimental

### 2.1 Experimental techniques

Gold and gold-silver alloy clusters were produced by a laser vaporization source [7]. The impact of a pulsed  $\text{Nd}^{3+}$ -YAG laser onto a rod of an  $\text{Au}_x\text{Ag}_{1-x}$  alloy (four different compositions were employed, corresponding to  $x = 0.25, 0.5, 0.75$  and 1) creates a hot atomic plasma, thermalized by helium gas. This leads to the cluster growth which is quenched during a supersonic expansion at the exit of the source chamber. The size distribution of these so-formed clusters can be controlled by varying the helium gas pressure. The clusters and the alumina matrix are, then, codeposited on several kinds of substrate, depending on further measurements to be performed. Two quartz balances were used to measure and control the film thickness and also the volumic fraction of metal for each sample.

Direct measurements by alpha-step allowed to precisely determine the film thickness of these samples which were between 220 and 310 nm while the volumic concentrations of metal did not exceed 3.6% in the samples with alloy clusters. However, for the sample containing pure gold clusters, the concentration reached 8.6% and the film thickness 390 nm. The size distributions were deduced from transmission electron microscopy (TEM) micrographs over a population of 750 to 1500 clusters per sample. The micrographs show clusters of roughly spherical shape and randomly distributed in the surrounding transparent matrix. The diameters ( $D_{max}$ ) at the maximum of the size distributions were determined to be in the size range 2 – 2.3 nm (Table 1). The absorption measurements were performed on films deposited on pure silica substrates with a Perkin-Elmer spectrophotometer. In order to compare the optical-absorption of one sample to another, the absorption coefficients were normalized with respect to the volumic concentration of metal.

The low-frequency Raman scattering (LFRS) spectra, from the composite films deposited on Si wafers, were recorded with a five-grating monochromator (Dilor Z40). The high rejection rate characterizing this set-up allows to measure Raman signal very close to the Rayleigh line. The light was detected by a photomultiplier with a GaAs photocathode. For the excitation, five different wavelengths were used: 457.9, 514.5 nm ( $\text{Ar}^+$  laser), 568.2, 647.1 and

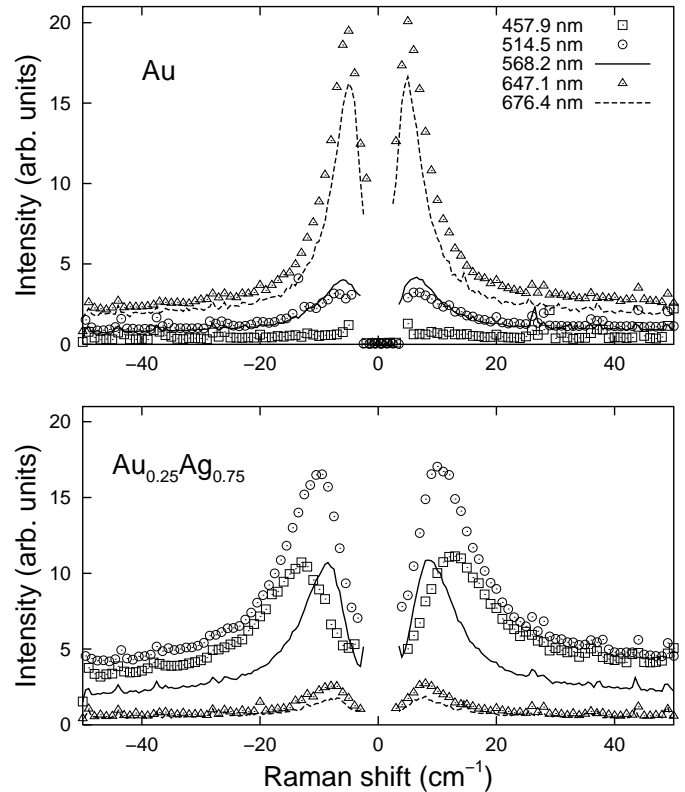


**Fig. 1.** Low-frequency Raman spectra obtained by excitation at different wavelengths, for Au and  $\text{Au}_{0.25}\text{Ag}_{0.75}$  nanoclusters.

676.4 nm ( $\text{Kr}^+$  laser). Experimental conditions like the excitation power, the incidence of the incoming beam on the sample, or the aperture of the slits of the monochromator, were kept the same. The signal detection was optimized as well as possible for all our measurements. In the discussion, normalized Raman intensities are implicit, *i.e.*, the measured Raman intensity divided by the film thickness, the volumic concentration of metal, and the photon flux depending on the excitation wavelength. Note that the spectral response of the spectrometer-photomultiplier system was also taken into account in the normalization of the Raman intensities.

### 2.2 Experimental results

The LFRS spectra from Au nanoclusters in alumina by excitation at different wavelengths are shown in Figure 1, and compared with the ones from  $\text{Au}_{0.25}\text{Ag}_{0.75}$  nanoclusters. The integrated intensity of the Raman peak and the absorption, as a function of the excitation wavelength, are superimposed in Figure 2, for different  $\text{Au}_x\text{Ag}_{1-x}$  compositions. Several observations are underlined. (1) The Raman intensity, for a same absorption, increases strongly with the Ag concentration in nanoclusters; (2) The excitation wavelength for the maximum of the Raman peak, like the absorption maximum, is shifted to the red with the increase of the Au concentration; (3) For an approximately same cluster size the Raman shift is smaller for the

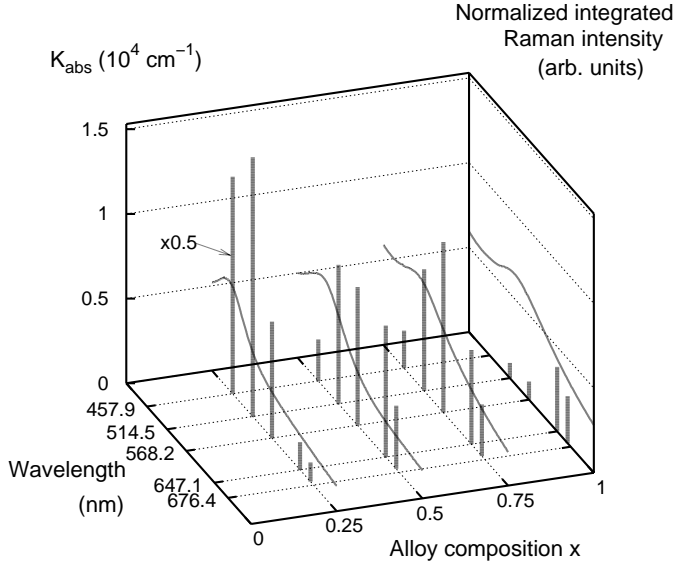


**Fig. 2.** Comparison of the integrated Raman intensities (vertical lines) with the absorption coefficients (smooth curves), for different incident light wavelengths and alloy composition  $x$ . The Raman intensities and the absorption spectra are normalized for a same absorption maximum. The Raman intensities corresponding to  $x = 0.25$  are divided by a factor 2.

Au nanoclusters; (4) The Raman shift decreases with increasing excitation wavelength, and more strongly for the  $\text{Au}_x\text{Ag}_{1-x}$  nanoclusters than for the Au ones (see Fig. 1). On the other hand, it is noted that only the Raman scattering by the quadrupolar modes corresponding to the quantum number  $\ell = 2$  is visible, as it was confirmed by the measurement of the depolarization ratio. As it will be shown in the following discussion, these experimental results prove that the effect of resonance of the Raman scattering is induced by the dipolar plasmon, and does not result from single core-electron excitations.

### 3 Discussion

For the quadrupolar vibrational modes, and the metallic studied nanoclusters, the relation between the frequency  $\omega$  and the cluster diameter  $D$  is the following [1,8,9]:

$$\omega(\text{cm}^{-1}) \simeq 0.85 \frac{v_t}{c D(\text{cm})} \quad (1)$$

where  $v_t$  is the transverse sound velocity in the alloy forming the cluster, and  $c$  the vacuum speed of light. It was shown [10] that  $I(\omega)\omega^\alpha \propto F(D)$ , where  $\omega$  and  $D$  are related by Eq. (1),  $I(\omega)$  being the Raman intensity and  $F(D)$  the cluster diameter distribution. The exponent  $\alpha$  depends on the spatial coherence in the cluster. It increases with the order or crystallinity. For the as-deposited Ag clusters investigated in [4], it was found  $\alpha = 0$ . After a thermal annealing, that improved the crystallinity,  $\alpha$  became close to 2 [10]. Due to the spatial coherence dependence of the Raman intensity, the frequency  $\omega_{max}$  at

the maximum of  $I(\omega)\omega^\alpha$ , is related to  $D_{max}$ , the diameter at the maximum of  $F(D)$ . Using the diameters determined by electron microscopy and the Raman intensities obtained by excitation at 514.5 nm (Table 1), Equation (1) is verified by taking  $\alpha = 2$ . For example, in the case of Au clusters, it is found  $v_t = 1158$  m/s with  $\alpha = 2$ , a transverse sound velocity which is close to the macroscopic one (1150 m/s), while with  $\alpha = 0$ ,  $v_t$  would be found two times smaller. This means that the order or crystallinity is much better in the investigated as-deposited Au or  $\text{Au}_x\text{Ag}_{1-x}$  clusters than in Ag ones.

The decrease of the Raman shift with the excitation wavelength was interpreted in a previous paper [4]. When the excitation is in the low-energy wing of the absorption band, the light absorption and the Raman scattering are due, for the most part, to the ellipsoidal prolate clusters in the composite film. The ellipsoidal prolate distortion splits the three-degenerate dipolar plasmon and the five-degenerate quadrupolar modes and red-shifts the non-degenerate plasmon and vibrational mode resulting from the respective splittings. As, by excitation of the non-degenerate dipolar plasmon, the effect of resonance occurs for the Raman scattering by the non-degenerate quadrupolar mode [4], a decrease of the Raman shift appears when the excitation is shifted to the red.

The change of the Raman intensity with the cluster composition is very interesting, because it brings informations on the effect of resonance. In *composite alumina*:  $\text{Au}_x\text{Ag}_{1-x}$  film, the surface plasmon energy increases with the Ag concentration, from approximately 2.35 eV ( $\lambda = 530$  nm) for Au clusters, to 2.95 eV ( $\lambda = 420$  nm) for Ag clusters. On the other hand, the conduction-electron (dipolar plasmon) and the core-electron (interband transition) excitations overlap decreases with the Ag concentration. Due to this overlap, there is a mixing of both excitations, and a decrease of the contribution of the conduction-electron excitation at the maximum of absorption spectrum [11]. For the Au clusters the absorption maximum is at 530 nm. The Raman scattering intensity is maximum by excitation at 647.1 nm, and zero at 457.9 nm in the interband transition spectral range (Figs. 1 and 2). It means that there is no resonant Raman effect when only the core-electron excitation is involved, and that the resonant Raman effect is maximum by excitation at lower energy than the one at the absorption maximum. From Fig. 2, the excitation wavelength for the maximum of Raman scattering shifts to the blue with the increase of Ag concentration in alloyed clusters, like the one for the absorption maximum.

Actually, homogeneous and inhomogeneous effects (their respective importance depend on the composition  $x$ ) have to be taken into account in order to explain the experimental data: (1) The resonant nature of the observed Raman signal requires the excitation of the surface plasmon, and the Raman signal is thought to be enhanced in the low energy side of the band because the contribution of the core-electron excitations (assumed to be not coupled to the quadrupolar vibrational modes) is relatively less important; (2) The composite films contain a

noticeable amount of non-spherical clusters, which have a low energy surface plasmon absorption band below the interband-transition spectrum because of the splitting of the three-degenerate plasmon by the quadrupolar distortion. This second effect (referred to as an inhomogeneous one) is more important for pure gold or gold-rich clusters, in which the mixing of conduction and core electron excitations at the dipolar plasmon frequency is strong: The integrated Raman signal is small and its maximum (as a function of the excitation photon energy) differs largely from the maximum of the recorded absorption spectrum of the film, because the Raman signal comes from a small number of strongly distorted clusters. Conversely, for silver-rich cluster compositions, the first effect (referred to as a homogeneous one) is more important: The integrated Raman signal is larger and its maximum closer to the absorption peak maximum (relatively to the case of gold-rich clusters) because the mixing with the interband transitions in the vicinity of the plasmon frequency is less pronounced (in the absence of a theoretical model for the dielectric function of the alloy, it is a reasonable assumption when interpolating between the cases of pure silver and pure gold metals) and consequently, a larger number of clusters contribute significantly to the Raman signal.

The resonant Raman scattering can be considered as a third order coherent process. (1) The incident light induces a real electronic excitation (or an electric oscillating dipole), (2) the coupling of the excited electrons with a vibration creates or annihilates a phonon corresponding to this vibration, (3) the interaction of the created electronic dipole with the vacuum induces the transition to the ground electronic level with a created (Stokes scattering) or annihilated (antiStokes) phonon. It follows that the effect of resonance exists if the interaction of the vibration with the excited electrons is allowed and relatively strong. From group theory, the interaction of the dipolar plasmon with the spherical and the quadrupolar vibrational modes is allowed [4]. However the interaction with the quadrupolar modes is stronger than with the spherical one [5,4]. It is why only the quadrupolar modes are observed in Raman scattering by excitation of the dipolar plasmon. The core electrons can be excited in many different levels, and it is likely that in several of them the interaction of the electrons with the spherical or quadrupolar modes is allowed. However, it is reasonable to think that the electron-vibration interaction is much stronger for a collective electronic excitation than for a mono-electronic one. It is why no resonant Raman scattering is observed by core-electron excitation. Furthermore, when there is a mixing of the conduction-electron collective excitation

with the core-electron mono-electronic one, the larger the core-electron contribution, the stronger the quenching of the resonant Raman effect. Indeed, a part of the incident light will be absorbed by the ineffective core-electron excitation, and will be no more available for the dipolar plasmon excitation, which is Raman effective. These remarks on the resonant Raman effect explain the experimental observations.

## 4 Conclusion

The observation of the vibrational Raman scattering from Au and  $\text{Au}_x\text{Ag}_{1-x}$  nanoclusters embedded in alumina films confirms that only the quadrupolar vibrational modes are visible as previously observed for Ag. This observation is possible because of the effect of resonance with the surface dipolar plasmon excitation, that is a collective mode of the conduction electrons. Conversely, there is no resonant Raman effect with the core-electron excitation. Furthermore, the mixing of both electronic excitations diminishes the resonant Raman effect, like it does for gold nanoclusters.

## References

1. G. Mariotto, M. Montagna, G. Viliani, E. Duval, S. Lefrant, E. Rzepka, C. Mai, *Europhys. Lett.* **6**, 239 (1988).
2. M. Fujii, T. Nagareda, S. Hayashi, K. Yamamoto, *Phys. Rev. B* **44**, 6243 (1991).
3. M. Ferrari, L.M. Gratton, A. Maddalena, M. Montagna, C. Tosello, *J. Non-Cryst. Solids* **191**, 101 (1995).
4. B. Palpant, H. Portales, L. Saviot, J. Lermé, B. Prével, M. Pellarin, E. Duval, A. Perez, M. Broyer, *Phys. Rev. B* **60**, 17107 (1999).
5. J.I. Gersten, D.A. Weitz, T.J. Gramila, A.Z. Genack, *Phys. Rev. B* **22**, 4562 (1980).
6. B. Palpant, B. Prével, J. Lermé, E. Cottancin, M. Pellarin, M. Treilleux, A. Perez, J.L. Vialle, M. Broyer, *Phys. Rev. B* **57**, 1963 (1998).
7. E. Cottancin, J. Lermé, M. Gaudry, M. Pellarin, J.-L. Vialle, M. Broyer, B. Prével, M. Treilleux, P. Mélinon, *Phys. Rev. B* **62**, 5179 (2000).
8. H. Lamb, *Proc. Math. Soc. Lond.* **13**, 187 (1882).
9. E. Duval, A. Boukenter, B. Champagnon, *Phys. Rev. Lett.* **56**, 2052 (1986).
10. E. Duval, H. Portales, L. Saviot, M. Fujii, K. Sumitomo, S. Hayashi, *Phys. Rev. B* **63**, 075405 (2001).
11. J. Lermé, B. Palpant, E. Cottancin, M. Pellarin, B. Prével, J.L. Vialle, M. Broyer, *Phys. Rev. B* **60**, 16151 (1999).